JOURNAL OF GEOPHYSICAL RESEARCH, VOL. 106, NO. D11, PAGES 12,099–12,107, JUNE 16, 2001

Multiyear measurements of aerosol optical depth in the Atmospheric Radiation Measurement and Quantitative Links programs

J. J. Michalsky, J. A. Schlemmer, W. E. Berkheiser, J. L. Berndt, and L. C. Harrison

Atmospheric Sciences Research Center, State University of New York at Albany, Albany, New York

N. S. Laulainen, N. R. Larson, and J. C. Barnard

Pacific Northwest National Laboratory, Richland, Washington

Abstract. The U.S. Department of Energy funded the development of the multifilter rotating shadowband radiometer (MFRSR) as part of the Atmospheric Radiation Measurement (ARM) program. This seven-channel radiometer began operation at the first ARM site in 1992 and at the Department of Energy Quantitative Links (QL) sites in the fall of 1991; three of the QL sites continue to operate, although this program was discontinued after 1995. This paper describes the use of the MFRSR in acquiring aerosol optical depth data, including the in-field calibration procedure and a partial validation of this process. Multiyear measurements of aerosol optical depth from three of the sites indicate similar phasing of seasonal and interannual changes, but with notable differences in the magnitude of the aerosol optical depth. Published papers that use these aerosol data are highlighted, and public access to these and future data sets for scientific studies are explained.

1. Introduction

The Atmospheric Radiation Measurement (ARM) program was established to support improvements in the measurement and modeling of radiative transfer in Earth's atmosphere; further, these improvements are to lead to better parameterization of the physics of the atmosphere for incorporation into general circulation models [*Stokes and Schwartz,* 1994]. This program funded the development of the multifilter rotating shadowband radiometer (MFRSR) [*Harrison et al.,* 1994] with the goal of establishing a modest spectral measurement capability of downwelling total and diffuse horizontal and direct normal solar irradiance. These instruments are deployed at southern Great Plains (SGP) sites in Oklahoma and Kansas, at two north slope of Alaska (NSA) sites near Barrow, and at two tropical western Pacific (TWP) sites on Manus Island, Papua, New Guinea, and the island nation of Nauru.

The Quantitative Links (QL) program was initiated to relate measured changes in atmospheric composition to changes in radiative fluxes that could lead to long-term changes in global temperature. Measurements were made at nine stations in the northeastern sector of the lower 48 United States for, at least, 4 years, with measurements continuing to this day at three of the sites (see Table 1).

Although the MFRSR data may be used in several ways and the QL program made measurements other than MFRSR measurements, the focus of this paper is on multiyear retrievals of aerosol optical depth using MFRSR data. Many of the problems and solutions discussed in this paper are applicable to standard Sun photometer measurements.

Paper number 2001JD900096.
0148-0227/01/2001JD900096$09.00

2. Calibration

The key to successful aerosol optical depth measurements is to develop a procedure to calibrate the radiometer on a quasi-continuous basis to the accuracy that is required. Our target accuracy for this study was ±0.01 optical depths. To assess what is required for the accuracy of our calibration constants, we express the Bouguer-Lambert-Beer law in instrument terms, namely,

$$V(\lambda) = V_o(\lambda)\exp[-\tau(\lambda)m], \quad (1)$$

where V and V_o are the responses of the radiometer at the surface and at the top of the atmosphere, respectively; τ is the total column optical depth due to scattering and absorption; and m is the air mass traversed by the direct solar beam relative to the air mass in the zenith direction. Hereafter, the wavelength dependence will be suppressed for clarity. It is to be understood that V_o is adjusted at any point in time to the correct solar distance. A propagation of error analysis leads to

$$(\Delta\tau)^2 = (\Delta V_o / mV_o)^2 + (\Delta V / mV)^2. \quad (2)$$

Since the error associated with the surface measurement V is only a one-half count of roundoff out of typically 1000-3000 counts, the second term is negligible relative to the first, therefore

$$\Delta\tau = \Delta V_o / mV_o. \quad (3)$$

To achieve an accuracy of 0.01 optical depth at one air mass, the error in V_o must be 1%.

Shaw [1976] discusses a number of contributions to errors in Sun photometry, including the problem of time variability of the aerosol optical depth. He points out that under certain circumstances a Langley plot of $\ln(V)$ versus m may appear linear, when, in fact, aerosol optical depth is changing, thus leading to a poor estimate of V_o. His suggestion was to calibrate when there are anticyclonic conditions, on mountain tops, in the morning before significant convection begins. *Reagan et al.* [1984, 1986]

Table 1. Quantitative Links Site Information and Data Record

Institution	Latitude, deg	Longitude, deg	Elevation, m	Available Data	Nearby City
Bluefield State College	37.26	-81.24	823	Nov. 1991 – present, minor gaps	Bluefield, W.Va.
Cornell University	42.40	-76.65	503	Oct. 1991 – Sep. 1995, major gaps	Ithaca, N.Y.
Illinois State Water Survey	40.05	-88.37	212	Nov. 1991 – June 1995, major gaps	Champaign, Ill.
Miami University	39.53	-84.72	285	Nov. 1991 – June 1995, minor gaps	Oxford, Ohio
NOAA ATDD	35.95	-84.28	380	Nov. 1991 – July 1997, major gaps	Oak Ridge, Tenn.
Penn State University	40.72	-77.93	375	Nov. 1991 – present, minor gaps	State College, Pa.
State University of New York at Albany	42.70	-73.83	85	Dec. 1991 – present, one major gap	Albany, N.Y.
University of Delaware	38.77	-75.10	13	Nov. 1991 – April 1996, major gaps	Lewes, Del.
University of Maine	45.21	-68.71	67	Oct. 1991 – April 1996, minor gaps	Orone, Maine

NOAA ATDD is the National Oceanic and Atmospheric Administration's Atmospheric Turbulence Diffusion Division.

further discuss the problem of obtaining a Sun photometer calibration using Langley plots and the problem of deciding when the aerosol optical depth is constant so that the V_o is acceptable. Their solution was to average the Langleys from the very best days in their data sets. Both *Shaw* [1976] and *Reagan et al.* [1984] make the further point that after a good Langley calibration is obtained, then the radiometer stability may be tracked using a stable calibration lamp. Although, in principle, calibration based strictly on standard lamps is a possibility, these have 2-3% uncertainty even with the most careful transfer of calibration from primary standards [*Kiedron et al.*, 1999] and will not meet our 1% accuracy target.

At our QL sites we did not have the resources to maintain calibrations based on frequent trips to a clean mountain site such as Mauna Loa. Furthermore, two of the filters in the 600 to 700-nm range in the MFRSR showed serious degradation over relatively short periods of time, and even semiannual trips to Mauna Loa would not suffice to capture the details of the change so that we could correct these data. Instead, we adopted a strategy for using the available Langley plots (Langleys) obtained on site to constantly update the calibration.

Our procedure is to process the 20 nearest successful Langley plots in time for an estimate of the calibration constant V_o, normalized to the average solar distance. Successful Langley plots using morning and/or afternoon data are selected using the objective algorithm developed by *Harrison and Michalsky* [1994], although other techniques can be used. Generally, days with a clear view of the solar disk, over an air mass range of two to six with little change in aerosol optical depths, led to apparently successful Langley plots. We then use a procedure based on the work of *Forgan* [1988] to winnow these 20 to 10. These 10 are selected by ratioing the V_o values of our 500-nm filter to those of the 862-nm filter and selecting the interquartile range of these ratios (see Figure 1). The mean of these 10 V_o is used to calculate optical depths for that day. Since the V_o calculated in this way is expected to vary slowly from instrument degradation caused by soiling of the diffuser or filter transmission changes and because this procedure cannot be applied at the beginning and end of a given deployment window, some smoothing of these results is used to interpolate within the time boundaries of a given deployment epoch and extrapolate near the ends. We use a lowess [*Cleveland*, 1979] smoother, but other techniques could be invoked. This process is illustrated in Figure 2. The squares are successful Langleys. The circles are based on the Forgan technique using 20 Langleys at a time, then incrementing by one Langley event at a time until we get to the last 20. The circles are positioned at the mean time of the 20 events. The smooth is through the Forgan points plus the 10 points at the beginning and 10 points at the end of an instrument deployment window.

Two additional procedures were evaluated in estimating a calibration constant for each filter. A very simple method is to use the median of a group of Langley events that are near in time to the day for which a V_o is required, say, 20 to 30 events. Another procedure is based on using a median calibration constant and then calculating time series of optical depths for the nearby Langley events to determine which have moderately constant optical depths during the range of air masses used for the Langley plots. These are then averaged. This last procedure is not independent of the former, therefore it should not be surprising that

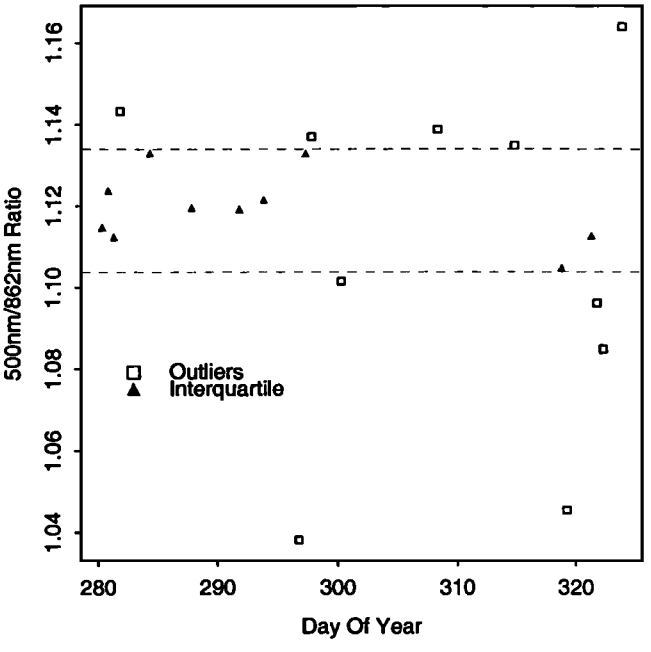

Figure 1. Illustration of the *Forgan* [1988] ratio Langley technique for choosing Langleys to use for surface measurement V_o determination.

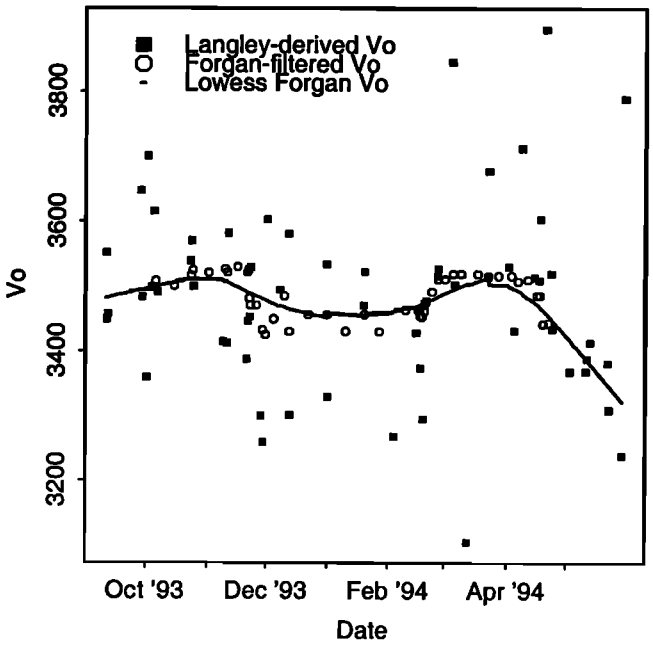

Figure 2. Multifilter rotating shadowband radiometer (MFRSR) deployment window. The 500-nm V_o from Langleys (squares) show the most scatter; the Forgan filtered V_o (circles) show much less scatter; and the lowess estimate (curve) is used in the final analysis to both smooth the Forgan results and provide estimates at either end of the configuration window.

the means are consistent with the medians. Both procedures agree with the ratio Langley technique to within 1% at all wavelengths. It should be mentioned that *Erxleben* [1998] discusses a clever extension of the Forgan technique that appears to return stable V_o.

As a related aside, it has been argued that choosing any reasonable V_o and calculating time series of optical depths should allow one to pick the stable aerosol days for use in Langley calibrations. Figure 3 demonstrates that this is not the case. The middle points are the aerosol optical depths based on the V_o obtained using the ratio Langley technique. The top and bottom curves are obtained by adding and subtracting 2% from this V_o. Figure 3 includes an afternoon's data between the air masses of 2 and 6 (note the top axis label), the range that we would typically use for a Langley plot. Even with a guess of V_o within 2% of what we believe is the true value, the bottom curve indicates a significant increase with time (air mass) that would eliminate these, otherwise, reasonable data from being considered for use in calibration. On the other hand, a time series of optical depths that appears very stable could be obtained from an incorrect V_o. Figure 3 also demonstrates that there is variability on the scale of a few thousandths of an optical depth even on a very clean day at the SGP site; note that the aerosol optical depth at this wavelength near 500 nm is only 0.04. Further, the error in optical depth behavior associated with errors in V_o, as discussed in regard to (3), is demonstrated by this figure, where the differences are ~ 0.01 at air mass 2 and decrease with increasing air mass.

The V_o calculated using the *Forgan* [1988] ratio Langley selection procedure has a formal statistical error of < 1%, in general, for the MFRSR based on an analysis of the 10 days selected from the interquartile range. That its true uncertainty is near this is based on a comparison of our aerosol optical depths with other Sun photometers during the ARM 1997 Aerosol Intensive Observation Period (IOP). In that study, four Sun photometers were compared including two measurements based on calibrations obtained directly or indirectly from Mauna Loa, Hawaii [*Schmid et al.*, 1999]. The root-mean-square difference of the MFRSR aerosol optical depths compared with the instrument that had been calibrated 2 weeks before the IOP at Mauna Loa was ~ 0.013 or less, consistent with a 1% error in the MFRSR and a 0.5% error in the Mauna Loa-calibrated instrument.

3. Multiyear Aerosol Optical Depth

Having derived a calibration V_o for each filter of the MFRSR, a straightforward application of (1) allows us to solve for the optical depth τ. Five of the filters of the MFRSR are selected to sample outside the influence of molecular water and oxygen

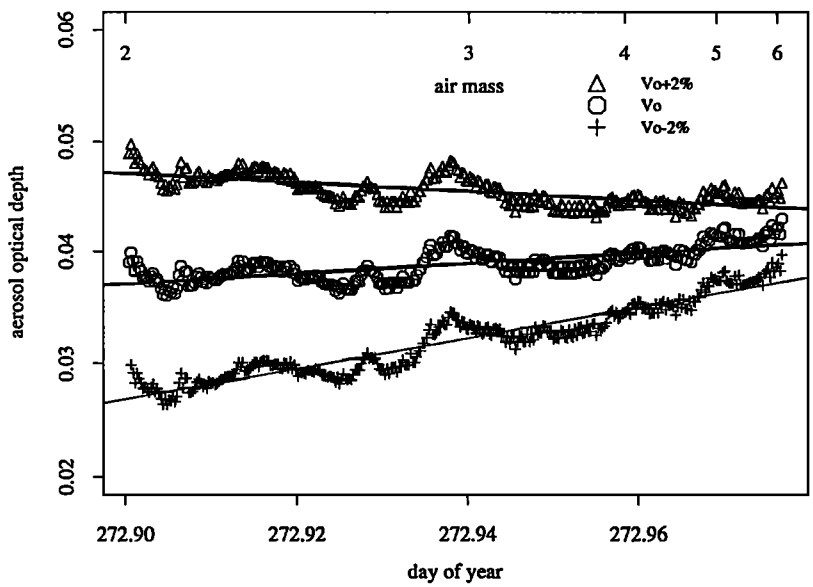

Figure 3. Time series of calculated aerosol optical depths at 500 nm using the best estimate of V_o (circles) and values of V_o that are 2% higher (triangles) and 2% lower (pluses).

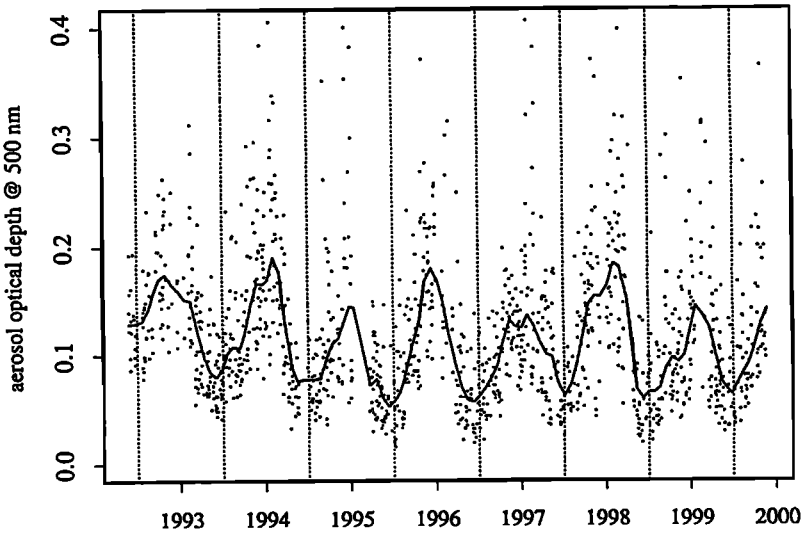

Figure 4a. Daily averaged aerosol optical depth at 500 nm with smoother applied to show seasonal and interannual variability from Oklahoma. Note summer peaks and winter minima.

bands, but they require a Rayleigh scattering optical depth and a Chappuis ozone band absorption optical depth subtraction to derive aerosol optical depth. We use the Rayleigh optical depth formulation of *Hansen and Travis* [1974]

$$\tau = 0.008569\lambda(1+0.0113\lambda+0.00013\lambda)P/P_o, \quad (4)$$

where λ is in micrometers, and we correct to the average pressure P at the site relative to sea level pressure P_o. A more precise correction would use a pressure measurement, which was not available at most of these sites. The ozone optical depth uses the absorption coefficient tables developed by *Shettle and Anderson* [1995] for the Chappuis and Wulf ozone bands in the visible and near-infrared. We used the ozone column abundance from the Total Ozone Mapping Spectrometer (TOMS) Web site for sites with data (toms.gsfc.nasa.gov) and the monthly mean ozone from the nearest Dobson site, otherwise (www.cmdl.noaa.gov/dobson). If we assume that the pressure varies by 10 mb from our standard pressure assignment and that temperature, humidity, and pressure profiles and therefore Rayleigh optical depths assume the range outlined by *Bucholtz* [1995], then an uncertainty of ~ 0.004 should be added to our shortest and most sensitive wavelength near 415 nm. Longer wavelengths will be much less uncertain from these effects. Uncertainty of 10 Dobson units in total column ozone will have the largest effect on the 610-nm optical depth, where it adds < 0.002 uncertainty.

Clear, 30-min periods are selected from the time series of optical depths generated from (1) using the estimated V_o, corrected for solar distance, for a given day, by fitting a linear function to the time series. If a single point in the series deviates by > 0.01 optical depth from this fit, we consider this an indication of a cloud. The fit is then performed on the 30-min times series formed by deleting the first point and adding the next point in the 30-min time series. Once the 0.01 optical depth deviation test is passed, the data are averaged and the time series incremented by 30 min for the next test. This is a conservative test designed to eliminate even modest subvisual cirrus effects. In fact, it proba-

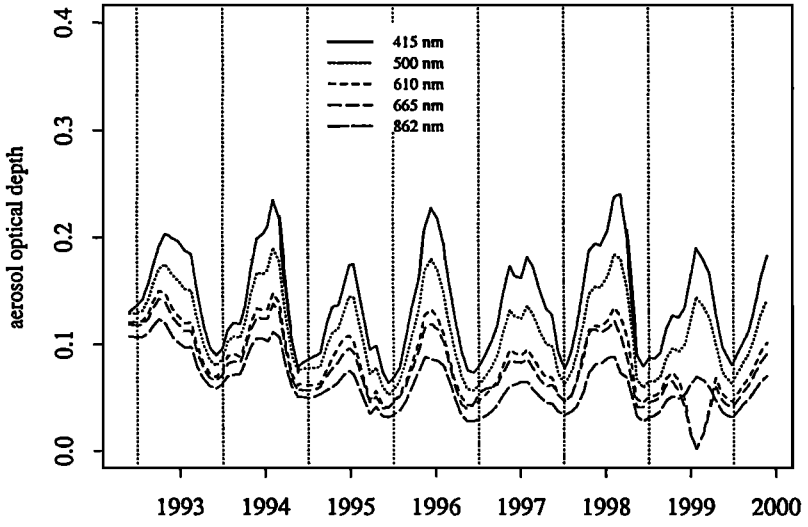

Figure 4b. Smoothed time series of aerosol optical depths for five wavelengths from Oklahoma. Note that optical depth decreases with wavelength.

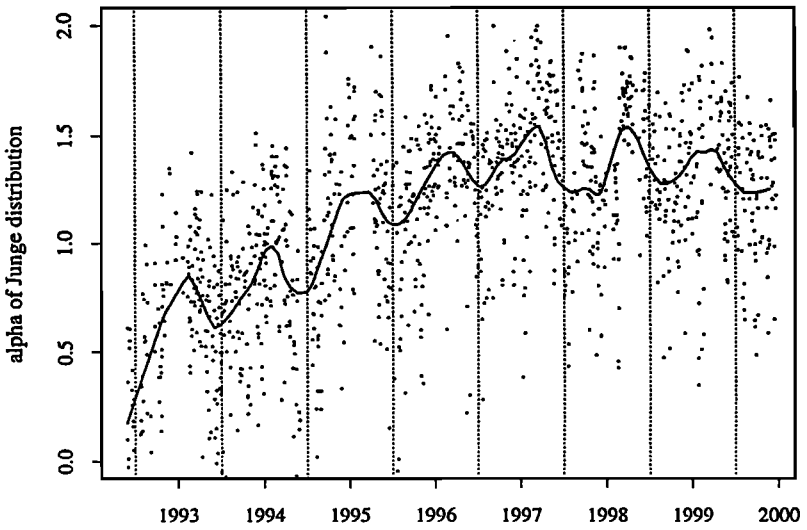

Figure 4c. Wavelength dependence of the aerosol from Oklahoma using the wavelength exponent in the equation $\tau = \beta\lambda^{-\alpha}$. Note the general decrease in particle sizes over the years and the winter and summer differences with larger aerosol in the winters.

bly eliminates some periods that are simply experiencing large changes in aerosol with no clouds around.

Figure 4a is a time series plot of aerosol optical depth for the filters near 500 nm for six different MFRSR configurations used in obtaining > 7 years of measurements at the ARM SGP site in northern Oklahoma. Each MFRSR has filters near the nominal wavelength assignments, but there are typically slight differences of a nanometer or so among the different MFRSR heads. Aerosol optical depths higher than ~ 0.40 are not plotted so as not to compress the scale more than it is; ~ 20 out of > 1185 points are not shown. Each point represents the daily average of the 30-min averages. A clear day may have many 30-min averages, but a hazy day may only have one or two; however, our purpose is to represent seasonal behavior, so we use the daily average in order that clear, clean days do not receive, in effect, more weight. There are ~ 175 daily averages, i.e., nearly a point every other day, obtained for a typical year in Figure 4a with points reasonably distributed throughout the year. The only significant gap is a 2-month period in 1995 that was caused by damage to the MFRSR's electronics by a near lightning strike. The solid line is a lowess [*Cleveland*, 1979] smoother through the data to help the eye visualize the seasonal and multiyear trend in aerosol optical depth. The lowess process smoothes, using a moving linear fit, over a 3-month window of data, with the points closest in time to the center of the window given significantly more weight. A second fit is done with an additional weight assigned according to the distance in optical depth of the points from the fit, which assigns less weight for distant points so as not to distort the smoothing caused by outliers.

Observe that the summer values are typically 2 to 3 times the winter values at the ARM SGP site. Summer aerosol optical depths show more interannual variability than winter ones, with the latter reaching almost the same minimum each year. The winter minima were higher for the first two winters because sig-

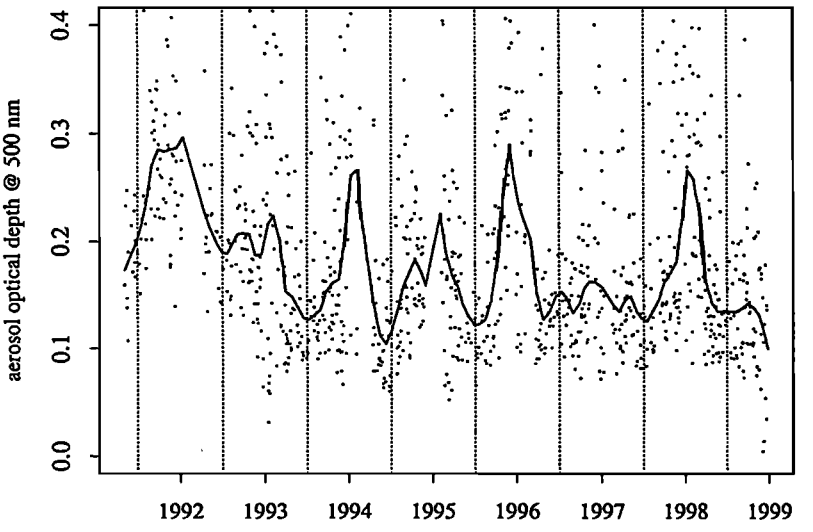

Figure 5a. Daily averaged aerosol optical depth at 500 nm with smoother applied to show seasonal and interannual variability from Pennsylvania State University (Penn State). Note summer peaks and winter minima.

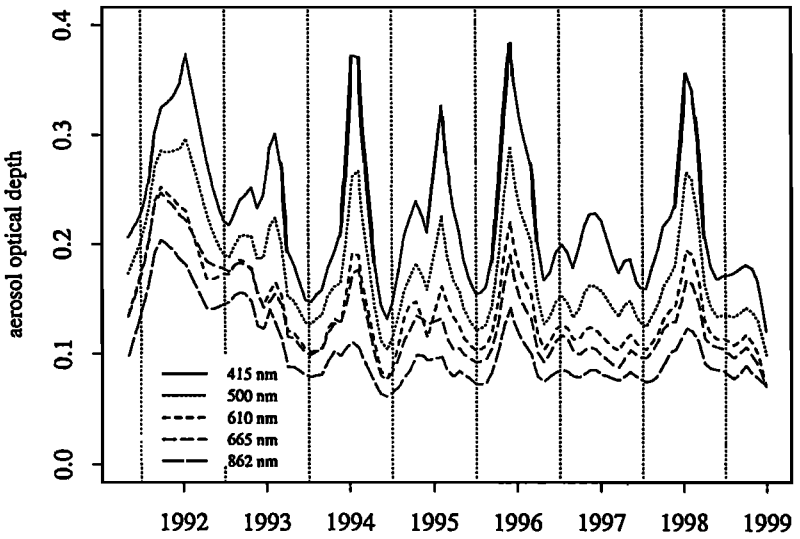

Figure 5b. Smoothed time series of aerosol optical depths for five wavelengths from Penn State. Note that optical depth decreases with wavelength.

nificant Mount Pinatubo aerosol remained in the stratosphere for a few years after its eruption in 1991 [*Russell et al.*, 1996].

Figure 4b contains the lowess fit to the same data set as in Figure 4a, along with four additional lowess fits to the data from the four other aerosol filters of the MFRSR. Generally, the shorter the wavelength, the higher is the optical depth; the only exceptions are marginal crossovers of the adjacent wavelength 610- and 665-nm filters during a few episodes over the 7-year span. Since these two filters are near in wavelength, aerosol optical depths are nearly the same. Both are affected by ozone, therefore errors in the estimated total column ozone combined with errors in the assigned ozone absorption coefficients plus the lowess interpolation process could be responsible for the slight crossovers. The correlation in optical depth from filter to filter is high, as can be seen by inspection, but there is some change is the wavelength dependence seasonally and over the 7-year period. To examine this, we make the assumption that the aerosol size distribution generally follows a power law. *Junge* [1963] demonstrated that this would lead to an aerosol optical depth that can be approximated by *Angstrom's* [1929] empirically determined relationship

$$\tau(\lambda) = \beta\lambda^{-\alpha}, \tag{5}$$

where τ is the aerosol optical depth, λ is the wavelength in micrometers, and β and α are constants determined by least squares fitting in natural log coordinates at the five wavelengths of the MFRSR. In general, (5) provides a good approximation to the wavelength dependence, with exceptions on a few very clear days where the fit is poor either because errors are fractionally higher or the size distribution deviates from the *Junge* [1963] power law. Figure 4c is a plot of the exponent α for each daily average and the lowess fit to these points using a 6-month window to examine size changes throughout the period. For very small particles, α approaches the value 4 (the Rayleigh scattering wave-

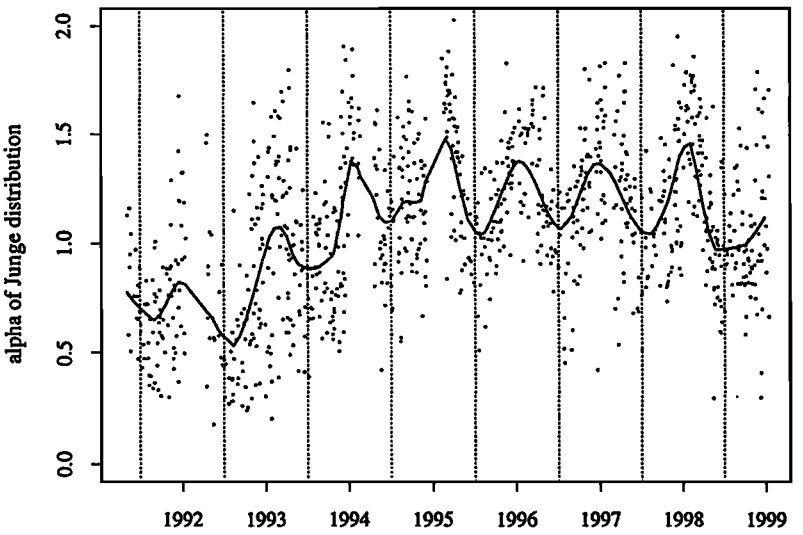

Figure 5c. Wavelength dependence of the aerosol from Penn State using the wavelength exponent in the equation $\tau = \beta\lambda^{-\alpha}$. Note the general decrease in particle sizes over the years and the winter and summer differences with larger aerosol in the winters.

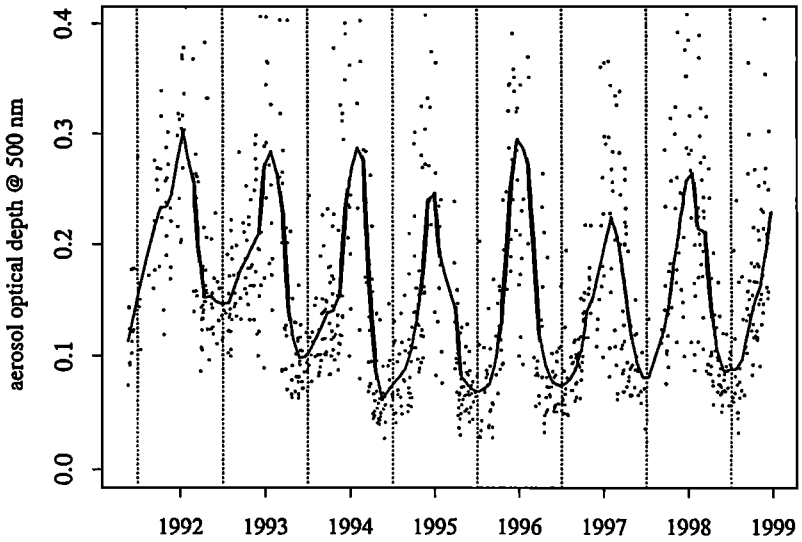

Figure 6a. Daily averaged aerosol optical depth at 500 nm with smoother applied to show seasonal and interannual variability from Bluefield State College. Note summer peaks and winter minima.

length dependence) and the value 0 for particles much larger than the wavelength of light. For continental aerosols a value of α around 1.3 is often measured, which is close to the average in the years after 1996. Before that, α was smaller, indicating the influence of large particles in the stratosphere that were only slowly removed after the Pinatubo eruption in 1991. The other notable feature is a seasonal pattern with slightly larger particles in the winter than in the summer.

Table 1 contains site information regarding the Quantitative Links network. Besides the MFRSR measurements, ancilliary instruments measured ambient temperature, relative humidity, and downwelling infrared irradiance, and a silicon pyranometer was pointed at the surface for the purpose of detecting snow. The MFRSR contained a total of seven filters, although we only discuss the data from five of these. One filter is centered on the strong water vapor band near 940 nm, and retrieval of total column water vapor using this filter is discussed elsewhere [*Michalsky et al.*, 1995]. The seventh filter is an unfiltered silicon sensor. Using it to approximate broadband shortwave radiation is discussed by *Zhou et al.* [1995].

Figures 5a-5c and 6a-6c contain plots similar to Figures 4a-4c from Rock Springs, Pennsylvania, and Bluefield, West Virginia, respectively, which are two of the sites from the QL network still in operation. Pennsylvania State University data in Figures 5a-5c are plotted on the same scale as Figures 4a-4c to facilitate comparisons. Figures 5a and 5b indicate that the Penn State site is generally more aerosol ladened than the Oklahoma site, with generally higher summer peaks and higher winter minima. The winter minima decrease after Pinatubo, and they have similar values after that. The summer maxima indicate a more complex behavior than the simple structure of the Oklahoma summer aerosol burdens, with the summer of 1997, for example, not much different than the preceding and succeeding winter. The wavelength dependence shown in Figure 5c is similar to that in

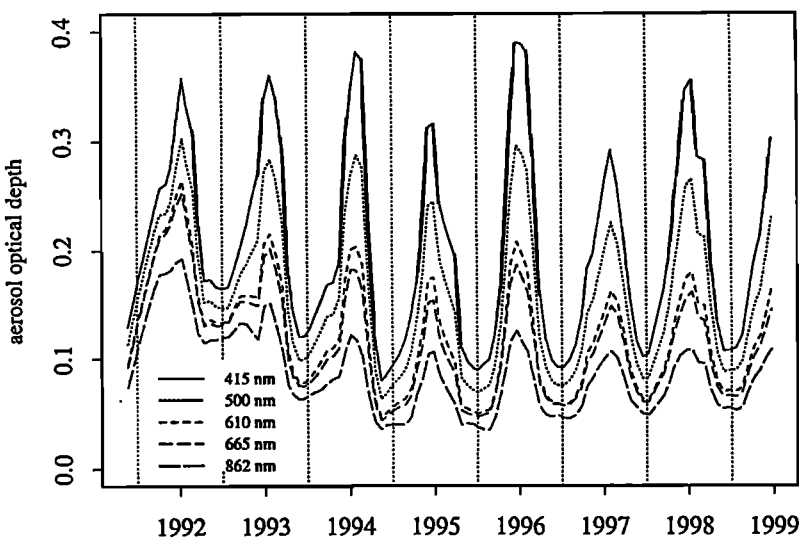

Figure 6b. Smoothed time series of aerosol optical depths for five wavelengths from Bluefield. Note that optical depth decreases with wavelength.

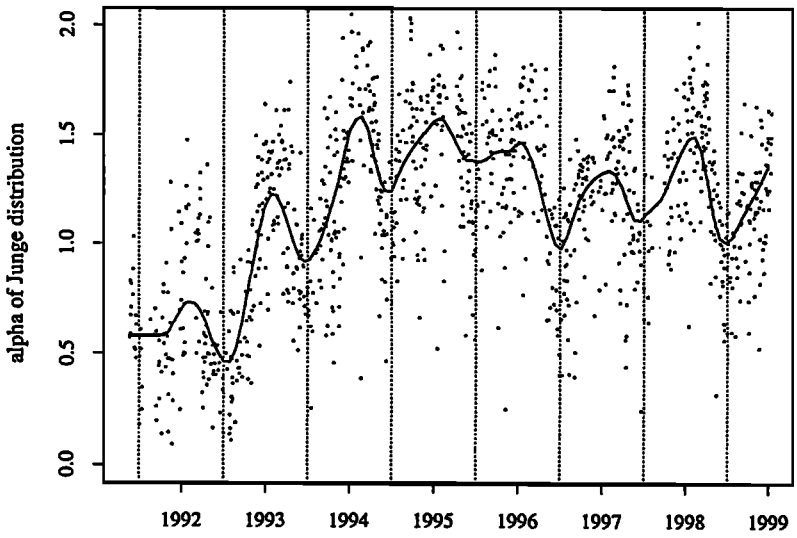

Figure 6c. Wavelength dependence of the aerosol from Bluefield using the wavelength exponent in the equation $\tau = \beta\lambda^{-\alpha}$. Note the general decrease in particle sizes over the years and the winter and summer differences with larger aerosol in the winters.

Figure 4c, with the recovery from Mount Pinatubo aerosol appearing sooner, probably because the higher aerosol burden near Penn State dominates the stratospheric contribution.

Figures 6a-6c contain similar plots for Bluefield, West Virginia. The summer peaks are similar to the highest Penn State data of Figures 5a-5c, but the winter minima at Bluefield are lower than at Penn State. After the recovery from Mount Pinatubo, the annual pattern over Bluefield is the most regular of the three sites. Again, the wavelength dependence looks similar to the other two sites, with winter minima and summer maxima indicating larger particles in the winter.

The QL funding was discontinued in 1995, when we closed three sites near Ithaca, Champaign, and Oxford. We continued to operate three other sites at Lewes, Orono, and Oak Ridge until their equipment failed over the next few years. Not shown are the data from Albany, which are slightly cleaner that those shown in Figures 5a-5c and 6a-6c.

4. Concluding Remarks

Since we have determined the V_o for each filter for each instrument on a quasi-continuous basis and since we find that the filters' spectral shapes are stable, even though their transmission may decrease, we can use these V_o values to determine calibration constants for the instruments in terms of spectral irradiance per instrument output by convolving the measured filter responses with an extraterrestrial spectrum [e.g., *Gueymard*, 1995]. The 30-min, plus daily averaged aerosol optical depths and daily spectral irradiance may be found on the World Wide Web at the URL hog.asrc.cestm.albany.edu. These data will be updated once or twice a year as long as the sites remain operational.

Several researchers have already found these data useful for studies that involve the comparisons of clear-sky models and measurements. For example, *Kato et al.* [1997] used the MFRSR aerosol measurements at the ARM SGP site in their study of clear-sky, downwelling total shortwave irradiance, where measurements were compared to models using, among other inputs, total column aerosol optical depth. For this shortwave problem, aerosol and its properties are the most crucial inputs to the models.

In a related study, *Halthore et al.* [1997] compared direct normal irradiance measurements made with an absolute cavity radiometer at the ARM SGP site to MODTRAN [*Berk et al.*, 1989]. Since the measurement of direct irradiance made with this instrument is extremely accurate, the inputs to the MODTRAN model were critical, especially the aerosol optical thickness, which has the most influence in the clear-sky problem. MFRSR aerosol measurements were used to corroborate the aerosol input parameters used in the model.

Fu et al. [1998] conducted a study similar to that *of Halthore et al.* [1997], where direct normal irradiance was examined using absolute cavity radiometer-corrected pyrheliometer data and the Fu-Liou radiative transfer code [*Fu*, 1991; *Fu and Liou*, 1992; 1993]. In this case the aerosol optical depths used were those measured by the MFRSR at the ARM SGP site.

A previous paper [*Michalsky et al.*, 1994] describing some of the early QL data, mostly from QL sites other than the ones presented here, and using a different approach than this analysis, was presented at a conference 5 years ago. This paper updates the data with a new calibration approach that has been applied uniformly to all of the data at our Web site given above.

In this paper we discussed measurements of aerosol optical depth using the MFRSR, which measures total and diffuse horizontal irradiance and calculates direct normal irradiance by subtracting the measured quantities, dividing by the cosine of the solar zenith angle, and correcting for the angular response variation from perfect Lambertian behavior. Our procedure for quasi-continuous calibration of the extraterrestrial responses of the instrument that are needed for calculation of optical depth was outlined, and some validation based on comparisons of optical depth to other instruments calibrated on Mauna Loa was presented. Data covering several years from three sites were presented showing seasonal and interannual differences, as well as the influence of Mount Pinatubo years after its eruption. We concluded with examples of the use of these data by others and information for obtaining these data for other research purposes.

Acknowledgments. This research was supported by the U.S. Department of Energy's Atmospheric Radiation Measurements Program through grant DE-FG02-90ER61072 and the Quantitative Links Program, both within

the Environmental Sciences Division of the Office of Health and Environmental Research, Office of Science. PNNL is operated for the Department of Energy by Battelle Memorial Institute under contract DE-AC0676RLO 1830.

References

Angstrom, A., On the transmission of sun radiation and on dust in the air, *Geogr. Ann.*, 2, 156-166, 1929.

Berk, A., L. S. Bernstein, and D. C. Robertson, MODTRAN: A moderate resolution model for LOWTRAN7, Geophys. Dir., Phillips Lab., Hanscom Air Force Base, Mass., 1989.

Bucholtz, A., Rayleigh-scattering calculations for the terrestrial atmosphere, *Appl. Opt.*, *34*, 2765-2773, 1995.

Cleveland, W. S., Robust locally weighted regression and smoothing scatterplots, *JASA*, *74*, 829-836, 1979.

Erxleben, W. H., Advanced signal processing techniques for the analysis of solar radiometer data in the presence of temporally varying aerosol optical depth, Ph.D. thesis, Univ. of Ariz., Tucson, 1998.

Forgan, B. W., Sun photometer calibration by the ratio-Langley method, in *Baseline Atmospheric Program (Australia) 1986*, edited by B. W. Forgan and P. J. Fraser, pp. 22-26, Bur. of Meteorol., Melbourne, Aust., 1988.

Fu, Q., Parameterization of radiative processes in vertically nonhomogeneous multiple scattering atmospheres, Ph.D. thesis, Univ. of Utah, Salt Lake City, 1991.

Fu, Q., and K. N. Liou, On the correlated k-distribution method for radiative transfer in nonhomogeneous atmospheres, *J. Atmos. Sci.*, *49*, 2130-2156, 1992.

Fu, Q., and K. N. Liou, Parameterizations of the radiative properties of cirrus clouds, *J. Atmos. Sci.*, *50*, 2008-2025, 1993.

Fu, Q., G. Lesins, J. Higgins, T. Charlock, P. Chylek, and J. Michalsky, Broadband water vapor absorption of solar radiation tested using ARM data, *Geophys. Res. Lett.*, *25*, 1169-1172, 1998.

Gueymard, C., SMARTS, a simple model of the atmospheric radiative transfer of sunshine: Algorithms and performance assessment, *Publ. FSEC-PF-270-95*, Fl. Sol. Energy Cent., Cape Canaveral, 1995.

Halthore, R. N., S. E. Schwartz, J. J. Michalsky, G. P. Anderson, R. A. Ferrare, B. N. Holben, and H. M. Ten Brink, Comparison of model estimated and measured direct-normal solar irradiance, *J. Geophys. Res.*, *102*, 29,991-30,002, 1997.

Hansen, J. E., and L. D. Travis, Light scattering in planetary atmospheres, *Space Sci. Rev.*, *16*, 527-610, 1974.

Harrison, L., and J. Michalsky, Objective algorithms for the retrieval of optical depths from ground-based measurements, *Appl. Opt.*, *33*, 5126-5132, 1994.

Harrison, L., J. Michalsky, and J. Berndt, Automated multifilter rotating shadow-band radiometer: an instrument for optical depth and radiation measurements, *Appl. Opt.*, *33*, 5118-5125, 1994.

Junge, C. E., *Air Chemistry and Radioactivity*, Academic, San Diego, Calif., 1963.

Kato, S., T. P. Ackerman, E. E. Clothiaux, J. H. Mather, G. G. Mace, M. L. Wesely, F. Murcray, and J. Michalsky, Uncertainties in modeled and measured clear-sky surface shortwave irradiances, *J. Geophys. Res.*, *102*, 25,881-25,898, 1997.

Kiedron, P. W., J. J. Michalsky, J. L. Berndt, and L. C. Harrison, A comparison of spectral irradiance standards used to calibrate shortwave radiometers and spectroradiometers, *Appl. Opt.*, *38*, 2432-2439, 1999.

Michalsky, J. J., J. A. Schlemmer, N. R. Larson, L. C. Harrison, W. E. Berkheiser III, and N. S. Laulainen, Measurement of the seasonal and annual variability of total column aerosol in a northeastern U.S. network, paper presented at International Specialty Conference, Aerosol and Atmospheric Optics: Radiative Balance and Visual Air Quality, Air & Waste Manage. Assoc., Pittsburgh, Pa., 1994.

Michalsky, J. J., J. C. Liljegren, and L. C. Harrison, A comparison of sun photometer derivations of total column water vapor and ozone to standard measures of same at the Southern Great Plains Atmospheric Radiation Measurement site, *J. Geophys. Res.*, *100*, 25,995-26,003, 1995.

Reagan, J. A., I. C. Scott-Fleming, B. M. Herman, and R. M. Schotland, Recovery of spectral optical depth and zero-airmass solar spectral irradiance under conditions of temporally varying optical depth, paper presented at IGARSS '84 Symposium, Int. Geosci. And Remote Sens. Symp., Strasbourg, France, 1984.

Reagan, J. A., I. C. Scott-Fleming, and B. M. Herman, Effects of temporal variations in optical depth on the determination of the optical depth and solar constant from solar photometry, paper presented at Beijing International Radiation Symposium, Radiation Commission, International Assoc. Meteorol. Atmos. Sci., Beijing, 1986.

Russell, P. B., et al., Global to microscale evolution of the Pinatubo volcanic aerosol derived from diverse measurements and analyses, *J. Geophys. Res.*, *101*, 18,745-18,763, 1996.

Schmid, B., J. Michalsky, R. Halthore, M. Beauharnois, L. Harrison, J. Livingston, P. Russell, B. Holben, T. Eck, and A. Smirnov, Comparison of aerosol optical depth from four solar radiometers during the fall 1997 ARM intensive observation period, *Geophys. Res. Lett.*, *26*, 2725-2728, 1999.

Shaw, G. E., Error analysis of multi-wavelength sun photometry, *Pure Appl. Geophys.*, *114*, 1-14, 1976.

Shettle, E. P., and S. Anderson, New visible and near IR ozone absorption cross-sections for MODTRAN, in *Proceedings of the 17th Annual Review Conference on Atmospheric Transmission Models*, Publ. PL-TR-95-2060, edited by G. P. Anderson, R. H. Picard, and J. H. Chetwynd, pp. 335-345, Phillips Lab., Hanscom Air Force Base, Mass., 1995.

Stokes, G. M., and S. E. Schwartz, The atmospheric radiation measurement (ARM) program: Programmatic background and design of the cloud and radiation test bed, *Bull. Am. Meteorol. Soc.*, *75*, 1201-1221, 1994.

Zhou, C., J. Michalsky, and L. Harrison, Comparison of irradiance measurements made with the multi-filter rotating shadowband radiometer and first-class thermopile radiometers, *Sol. Energy*, *55*, 487-491, 1995.

W. E. Berkheiser III, J. L. Berndt, L. C. Harrison, J. J. Michalsky, and J. A. Schlemmer, Atmospheric Sciences Research Center, State University of New York at Albany, 251 Fuller Road, Albany, NY 12203 USA. (berk@asrc.cestm.albany.edu; jerry@asrc.cestm.albany.edu; lee@asrc.cestm.albany.edu; joe@asrc.cestm.albany.edu; jim@asrc.cestm.albany.edu.)

J. C. Barnard, N. R. Larson, and N. S. Laulainen, Pacific Northwest National Laboratory, P.O. Box 999, Richland, WA 99352 USA. (james.barnard@pnl.gov; nels.larson@pnl.gov; nels.laulainen@pnl.gov.)

(Received August 4, 2000; revised January 2, 2001; accepted January 19, 2001.)